Journal of Materials Chemistry B

PAPER

View Article Online
View Journal | View Issue



Cite this: J. Mater. Chem. B, 2014, 2, 181

# Enabling multi-enzyme biocatalysis using coaxial-electrospun hollow nanofibers: redesign of artificial cells

Xiaoyuan Ji,[ab] Ping Wang,[ac] Zhiguo Su,[a] Guanghui Ma[a] and Songping Zhang*[ad]

Highly efficient immobilization of multi-enzyme systems involving cofactor regeneration represents one of the greatest challenges in bioprocessing. Particulate artificial cells with enzymes and cofactors encapsulated within microcapsules have long been the major type of multi-enzyme biocatalysts. In the present work, a novel hollow nanofiber-based artificial cell that performs multi-step reactions involving efficient coenzyme regeneration was fabricated *in situ* by a facile co-axial electrospinning process. To that end, a mixture of glycerol and water containing the dissolved multi-enzyme system for the bile acid assay, which included 3α-hydroxysteroid dehydrogenase (3α-HSD), diaphorase (DP) and NADH was fed as the core phase solution, and a *N*,*N*-dimethylacetylamide solution of 30 wt% polyurethane was fed as the shell phase solution during the co-axial electrospinning. The relationship between the structures of the hollow nanofibers and the activity and stability of the encapsulated enzymes was studied. At core and shell phase electrospinning solution flow rates of 0.07 and 0.5 mL $h^{-1}$, activity recoveries as high as 76% and 82% were obtained for the encapsulated 3α-HSD and DP. The hollow nanofiber-based artificial cells were successfully used for the bile acid assay, yielding good linearity for bile acid concentrations ranging from 0–200 μM. Compared with the solution-based multi-enzyme system, the hollow nanofiber-based multi-enzyme system presented a lumped activity recovery of 75%. In addition, the hollow nanofiber provided the multi-enzyme system confined inside the nano-domain of the hollow fibers with a unique stabilizing mechanism, such that more than a 170-fold increase in half-life at 25 °C was obtained for the encapsulated 3α-HSD and DP. This study is expected to greatly promote and broaden the application of multi-enzyme systems in industry, biosensor, biomedical, and many other related research fields.

Received 5th September 2013
Accepted 21st October 2013

DOI: 10.1039/c3tb21232g

www.rsc.org/MaterialsB

## 1. Introduction

Biological cells that perform multi-step biochemical reactions constitute the crucial part of life. Reconstruction of the structure and function of biological cells by biomimetically incorporating multi-enzymes and the necessary coenzymes in a confined environment holds tremendous promise for biocatalysis,[1,2] bioassays,[3] and therapeutic applications, for example, as artificial organelles.[4,5] During past decades, studies have been heavily focused on encapsulating multi-enzymes that perform cascade reactions using polymeric semipermeable membranes,[1,2,6–9] natural liposomes,[10] capsosomes,[11,12] and polymeric vesicles, which are also known as polymersomes.[5,13–17] The multi-enzyme systems that have been reported so far are almost exclusively in discrete spherical capsules with single or multicompartments, with a few examples using porous supports[18,19] or nanoparticles.[20–23] Encapsulation of multi-enzyme systems, however, has limitations in some significant applications owing to the often complicated and non-biofriendly preparation process, enzyme deactivation upon direct contact with organic solvents, low loading capacity, and conflict between diffusion resistance and mechanical strength encountered in the optimization of the encapsulation process.

Advances in electrospinning techniques for fabricating nanofibers with a hollow interior structure for the formation of continuous non-woven membranes inspired us to redesign the conventional artificial cell for multi-enzyme biotransformations. Electrospinning two immiscible liquids through a coaxial, two-capillary spinneret, which was proposed by Loscertales *et al.*,[24,25] has been successfully adopted to directly fabricate several kinds of ceramic hollow nanofibers.[26–30] A typical set up for co-axial electrospinning is depicted in Scheme 1. By carefully choosing a bio-friendly solution with

[a]National Key Laboratory of Biochemical Engineering, Institute of Process Engineering, Chinese Academy of Sciences, Beijing 100190, China. E-mail: spzhang@home.ipe.ac.cn; Fax: +86 10-8254-4958
[b]University of Chinese Academy of Sciences, Beijing, 100049, PR China
[c]Department of Bioproducts and Biosystems Engineering and Biotechnology Institute, University of Minnesota, St. Paul, MN 55108, USA
[d]Collaborative Innovation Center of Chemical Science and Engineering (Tianjin), Tianjin, 300072, China

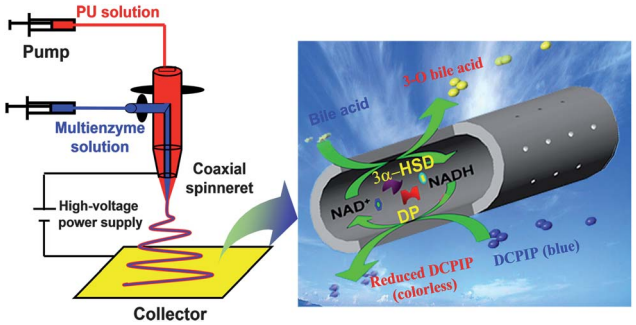


Scheme 1 Schematic illustrations of the setup for co-axial electrospinning (left) and the nanofiber-supported multi-enzyme artificial cells involving 3α-HSD, DP and NAD(H) for the bile acid assay (right).

dissolved multi-enzymes as the core solution and an immiscible solvent with dissolved polymer as the shell solution for the co-axial electrospinning, *in situ* encapsulation of multi-enzymes inside the nanodomain of the hollow nanofibers can be realized. Compared to the exiting encapsulated multi-enzyme systems that take the form of particulates, novel hollow nanofiber-supported artificial cells are expected to offer several advantages: the specially designed two-capillary spinneret will prevent the bioactive molecules from coming into direct contact with the organic solvent; the *in situ* encapsulation process ensures nearly 100% loading efficiency for expensive enzymes; the diffusion distance for reactants crossing the walls of the hollow nanofibers with nano-scale thickness is much reduced; molecular interactions between enzymes and possibly shared cofactors are facilitated, as well as enhancing the enzymes stability due to the confinement of the multi-enzyme system inside the nano-scaled compartments.[31,32] Furthermore, the woven-membrane formed from the electrospun nanofibers enables easy recycling and operation, and at same time the conflict between mechanical strength and mass transfer resistance encountered on optimization of the particle-based system will be avoided.

Highly efficient immobilization of multi-enzyme systems involving cofactor regeneration represents one of the greatest challenges in bioprocessing.[19,21] Herein, to demonstrate the feasibility and advantages of the proposed artificial cells supported by hollow nanofibers, a bi-enzymatic system for the bile acid assay, which includes 3α-hydroxysteroid dehydrogenase (3α-HSD), diaphorase (DP) and NAD(H) was constructed (Scheme 1). The essential translocation of the cofactor between 3α-HSD and DP will facilitate the simultaneous oxidation of bile acid and reduction of the blue dye 2,6-dichlorophenolindophenol (DCPIP) to its colorless reduced product, thus NAD(H) is regenerated and the signal for bile acid assay is magnified.

# 2. Experimental section

## 2.1 Reagents

Polyurethane A85E (PU) pellets with a bulk density of approximately 700 kg $m^{-3}$ was supplied by Xiamen Jinyouju Chemical Agent Co. (Xiamen, China). Diaphorase (DP, EC 1.8.1.4) and 3α-hydroxysteroid dehydrogenase (3α-HSD, EC 1.1.1.50) were supplied by Beijing Apis Biotechnology Co. (Beijing, China). Nicotinamide adenine dinucleotide ($NAD^+$ and NADH), bovine serum albumin (BSA), protamine, lysozyme, *N*,*N*-dimethylacetylamide (DMAc), fluorescein isothiocyanate (FITC), dimethyl sulfoxide (DMSO), trihydroxymethyl aminomethane (Tris) and glycerol were all purchased from Sigma.

## 2.2 Preparation of the PU hollow nanofiber encapsulated multi-enzyme system

The general procedure for preparing nanofiber based artificial cells for bile acid assay by co-axial electrospinning was as follows: the shell solution was prepared by dissolving PU in DMAc to get a final polymer concentration of 30 wt%, the core solution was prepared by mixing 950 μL glycerol with 50 μL ultra-pure water solution containing 1 mg 3α-HSD, 1 mg diaphorase, and 50 mg NADH. A spinneret containing two coaxial stainless steel needles was used. The inner and outer diameters of the core nozzle were 0.42 and 0.72 mm, and that of shell nozzle were 0.92 and 1.28 mm, respectively. The core solution and shell solution were fed at a constant rate through two syringe pumps. The feeding rate for the PU solution was set at 0.5 mL $h^{-1}$, the rate for core solution varied in the range of 0.05 to 0.2 mL $h^{-1}$. A positive voltage of 14–17 kV was applied and an aluminium sheet was used as the collector at a distance of 25 cm away from the nozzle tip. Electrospinning was carried out at 25 ± 3 °C, humidity 10–15%. After a stable electrospinning operation was carried out, nanofibrous membrane was collected every 30 min. The collected nanofiber membrane was stored overnight in a laminar hood at room temperature to evaporate the residual solvent.

## 2.3 Characterization

The viscosities of the electrospinning solutions at 25 °C were measured with a Rotator Viscosity Meter (DV-1, Shanghai Yueping Instrument Company, Shanghai, China). The morphologies of the fibers were characterized by scanning electronic microscopy (SEM, JSM-6700F, JEOL, Japan). To view a cross-section of the hollow nanofibers, the collected nanofibrous membranes were frozen in liquid nitrogen, and then cut perpendicularly to the axis of the fibers, exposing their hollow structure. To determine the size distribution of the inner and outer diameters of the prepared hollow PU nanofibers, approximately 100 different nanofibers were analyzed from the SEM images. The structures of the fibers were also characterized by transmission electron microscopy (TEM, JEM-2100UHR, JEOL, Japan).

In order to characterize the distribution of enzymes inside the lumen of the hollow nanofibers, fluorescein isothiocyanate labeled (FITC-labeled) 3α-HSD was encapsulated by co-axial electrospinning using DMAC solution with 30 wt% PU as the shell phase solution and 950 μL glycerol with 50 μL water solution of 1 mg 3α-HSD as the core phase solution at core–shell phase solution flow rates of 0.07 and 0.5 mL $h^{-1}$, respectively. Confocal laser scanning microscopy (CLSM) was used to characterize the hollow nanofibers containing encapsulated FITC-labeled protein using a Leica TCS SP5 microscope (Leica Camera AG, Germany).

 

The laser provided excitation of FITC at 488 nm, and emitted fluorescent light was detected between 500 and 545 nm.

The fluorescent labeling of 3α-HSD with FITC was carried out according to the following procedure: 50 mg of FITC dissolved in 8 mL DMSO was slowly added to 100 mL 0.2 M sodium phosphate buffer pH 8.0 containing 1 g 3α-HSD, the mixture was gently stirred at room temperature in the dark for 2 h, then excess FITC was removed by ultrafiltration centrifugation at 10 000 rpm. The fraction containing FITC-labeled 3α-HSD was then lyophilized at 6 °C and 0.12 mbar using a benchtop freeze-dryer (Beta 2–16 with LMC-2 system control, Christ, Osterode, Germany).

### 2.4 Enzyme activity assay for 3α-HSD and DP

From our preliminary tests, the activities of the buffer-washed and un-washed nanofiber membranes containing enzyme did not show a detectable difference because the final concentration of glycerol released into in the assay system was negligable. Therefore it was thought that the glycerol co-encapsulated inside the hollow nanofiber had no effect on the enzyme activity measurement, and in the following experiment, no washing step was performed before the enzyme assay. An activity unit of 3α-HSD was defined as the amount of enzyme needed to oxidize 1 μmol bile acid to 3-o-bile acid in 1 min at pH 8.0 and 25 °C. The activity of 3α-HSD was determined by measuring the initial oxidation rate of bile acid at 25 °C. To 1 mL Tris-HClbuffer solution (50 mM pH 8.0) containing bile acid (50 mM) and $NAD^+$ (1 M), free 3α-HSD (1 μg) or a piece of nanofibrous membrane (approximately 3 mg) containing approximately 3-α-HSD (1 μg) were added to initiate the reaction. The reaction was monitored by measuring the absorbance at 340 nm, $A_{340}$ ($\varepsilon^{NADH} = 6.22\ mM^{-1}\ cm^{-1}$), continuously for 5 min using a Unico 2800 spectrophotometer. For the activity measurement of the nanofibrous enzyme, $A_{340}$ was measured every 30 s after retrieving the fibers from the solution with tweezers.

The activity of DP was determined using a similar procedure, monitoring the disappearance of DCPIP in the reaction mixture. One unit of diaphorase was defined as the amount of enzyme needed to reduce 1 μmol DCPIP in 1 minute at pH 8.0 and 25 °C. Typically 1 μg free DP or a piece of immobilized DP was used in 1 mL Tris-HClbuffer (50 mM pH 8.0) containing DCPIP (0.04 M) and NADH (0.1 M) at 25 °C. The reaction was monitored by measuring $A_{600}$ ($\varepsilon^{DCPIP} = 19.1\ mM^{-1}\ cm^{-1}$) continuously for 5 minutes using a Unico 2800 spectrophotometer.

### 2.5 Standard curve for the bile acid assay

When the hollow nanofiber-based multi-enzyme system was used, approximately 4 mg nanofibrous membrane was added to 2 mL Tris-HClbuffer solution (50 mM, pH 8.0) containing 0.04 mM DCPIP and bile acid (0–400 μmol $L^{-1}$) to initiate the coupled reaction. The final enzyme concentrations were calculated to be as follows: 3α-HSD 0.7 μg $mL^{-1}$, DP 0.7 μg $mL^{-1}$ and NADH 0.05 mM. All assays were conducted at 37 °C, and changes in $A_{600}$ were continually monitored for 5 min. Control tests were carried out using blank hollow nanofibers prepared using a core solution containing no enzymes or coenzyme.

When the measurement was carried out using the free multi-enzyme system, or using co-immobilized 3α-HSD and DP with additional free NADH, the concentrations of enzymes and NADH were all adjusted to the same values as those in the above hollow nanofiber-based multi-enzyme system.

### 2.6 Release test for encapsulated substances in the hollow nanofibers

Seven different types of core solutions for co-electrospinning were prepared individually by dissolving 10 mg glycerol ($M_w$ 92.09), 10 mg NADH ($M_w$ 763.4), 10 mg protamine ($M_w$ 5000), 10 mg lysozyme ($M_w$ 14 000), 10 mg diaphorase ($M_w$ 24 000), 10 mg 3α-HSD ($M_w$ 30 000), or 10 mg BSA ($M_w$ 65 000) into a mixture of 950 μL glycerol and 50 μL ultra-pure water. With 30 wt% PU in DMAc as the shell solution, seven types of hollow nanofiber membranes containing encapsulated substances with molecular weights ranging from 92 to 65 000 Da were prepared *via* coaxial electrospinning at a core–shell flow rate of 0.07 : 0.5 mL $h^{-1}$. After achieving stable electrospinning operation, nanofibrous membrane was collected every 30 min.

To measure the release of each encapsulated substance from the hollow nanofibers, the membranes collected over 30 min were immersed in 5 mL pure water, and incubated at 25 °C with 150 rpm shaking. At different time intervals, the concentration of the encapsulated substance released into water was measured using an appropriate method and previously established standard curves. Specifically, the glycerol concentration was analyzed using an Agilent HPLC machine equipped with an Agilent Zorbax Carbohydrate Analysis Column and on-line UV-detector (270 nm). Acetonitrile–water (85 : 15, v/v) was used as the mobile phase at a flow rate of 1 mL $min^{-1}$. The NADH concentration was measured using a Unico 2800 spectrophotometer by measuring the absorbance at 340 nm, $A_{340}$ ($\varepsilon^{NADH} = 6.22\ mM^{-1}\ cm^{-1}$). The concentrations of protamine, lysozyme, diaphorase, 3α-HSD and BSA were measured using Bradford methods and previously established standard curves. The percentage release of each substance was defined as the ratio of the total released amount at different times to the total amount encapsulated in the hollow nanofibers.

The total amount of encapsulated substance in the hollow nanofiber prepared at the core–shell solution flow rate of 0.07 : 0.5 mL $h^{-1}$ was calculated as follows. The total weight of the nanofiber membrane collected after 30 min stable co-electrospinning was approximately 100 mg. Then, the total volume of electrospun core solution will be 0.035 mL (0.07 mL $h^{-1}$ × 0.5 h). Considering the concentration of substance in the core solution was 10 mg $mL^{-1}$, in total 0.35 mg of the substance was encapsulated inside the 100 mg membrane sample. Therefore, the amount of substance encapsulated was 0.0035 mg substance per mg nanofiber membrane. When 50 mg membrane was added to 5 mL pure water to measure release of the encapsulated substance, the percentage release was calculated from the following equation:

$$\text{Percentage release} = (\text{concentration of substance in water (mg mL}^{-1}) \times 5\ \text{mL})/(0.0035\ (\text{mg substance per mg membrane}) \times 50\ \text{mg membrane}) \times 100\%$$

### 2.7 Enzyme stability tests

The stabilities of 3α-HSD and DP were examined by monitoring changes in enzyme activity as a function of incubation time under desired conditions. Native enzyme samples were placed in 50 mM Tris-HCl buffer solutions (pH 8.0) or core solutions (95% glycerol + 5% water) and stored in an incubator with the temperature controlled in the range of 4 °C to 50 °C. Nanofiber-supported enzymes (3α-HSD, DP, and the multi-enzymes involving 3α-HSD, DP and NADH) were sealed in plastic Ziploc bags, and stored in the incubator with the temperature controlled in the range of 4 °C to 50 °C. The residual activities of the enzymes were measured periodically. For stability measurements of individually encapsulated 3α-HSD and DP, all other components were added outside.

The stability of the hollow nanofiber supported multi-enzyme artificial cells was examined by monitoring changes in coupled reaction rate as a function of storage time with the reaction rate of freshly prepared multi-enzymes system defined as 100%.

The stability of NADH in 50 mM Tris-HCl buffer solutions (pH 8.0) or core solution (95% glycerol + 5% water) at 25 °C was measured by monitoring the decrease in absorbance of the dihydropyridine at 340 nm as a function of incubation time.

## 3. Results and discussion

### 3.1 Preparation of hollow nanofibers *via* co-axial electrospinning

Nanofibers have been widely used as carriers for enzyme immobilization *via* surface attachment and encapsulation; both methods have been comprehensively reviewed recently.[33,34] Surface attachment will obviously limit the molecular interaction among enzymes and coenzymes, which is considered to be a decisive factor for efficient regeneration of the immobilized coenzymes. With regard to the encapsulation of enzyme in the nanofiber achieved by direct co-electrospinning of enzymes and other components (organic or inorganic materials), however, most of the enzyme molecules are confined inside the nonporous fibers. Consequently, not only is the accessibility of the substrate to the enzyme inhibited, but also the flexibility of the coenzymes is lost. Therefore, in the present study, we aim to fabricate a hollow nanofiber *via* a co-axial electrospinning technique to accommodate both enzymes and the shared coenzyme inside the lumen of the nanofiber, so that efficient molecular interaction among enzymes and coenzymes can be ensured or even facilitated.

To achieve a successful co-axial electrospinning process, selecting an appropriate combination of core and shell solutions was the most critical factor. Generally, immiscibility of core and shell solution was considered a premier requirement for well-defined coaxial-structured nanofibers,[35] although Sun *et al.*[36] claimed that core-sheath fibers could be produced by electrospinning two polymer solutions, where either the polymers or solvents were miscible. Co-axial electrospinning of two different polymer solutions usually generates a core-sheath structured nanofiber,[36–39] removing the core-polymer by selective dissolution or calcination is necessary to obtain a hollow fiber. By combining poly(vinyl pyrrolidone) (PVP) and $Ti(OiPr)_4$ in ethanol as a shell solution and mineral oil as a core solution, ceramic hollow nanofibers were obtained directly once the oil had been extracted from the core.[26–28] These techniques, however, are obviously not suitable for *in situ* encapsulation of bioactive molecules. Ideally, the core solution should be bio-friendly and not contain any polymers so that no post-treatment will be required.

Based on extensive screening, glycerol with a water content of less than 10 v/v% was found to meet the requirements of an ideal core solution, with which uniform hollow nanofibers of polyurethane (PU) could be successfully prepared by using 30 wt % PU in DMAc as the shell solution. Miscibility testing carried out by mixing the shell and core solvent showed that glycerol with a water content of up to 10 v/v% was very miscible with DMAc, but mixing glycerol with DMAc containing PU precipitated the PU and an opaque solution was formed after a long mixing period. This was likely because although glycerol is highly miscible with DMAc, both glycerol and water are non-solvents for PU, causing it to aggregate and precipitate. Despite this, and probably due to the diffusion rate of these two highly viscous solutions being slower than the electrospinning process, which allows a typical residence time in the Taylor cone of about 1 s,[35] a stable co-axial jet could be formed before the gelation of the outer liquid. However when the water content in the core solution was higher than 20 v/v%, formation of an elastic gel-like substance at the tip of the nozzle was observed, so that stable electrospinning was no longer possible. It was speculated that the viscosity of the core solution with high water content was much reduced, leading to faster diffusion of the two immiscible solutions and consequently immediate precipitation of PU upon contact with core solution in the jet. The viscosities of the electrospinning solutions are listed in Table 1. A similar observation was reported when DMSO was used as the core solvent with 20 wt% polystyrene in DMF as the shell phase solution.[35]

To obtain a compromise between a stable electrospinning process and good dispersion of the enzymes, glycerol containing 5 v/v% water was used as the core solution. By changing the flow rate of the core phase solution, nanofibers with different morphologies were obtained. Fig. 1 shows that at a fixed shell phase solution flow rate of 0.5 mL $h^{-1}$, formation of hollow fibers with continuous cylindrical channels was strongly dependent on the flow rate of the core phase solution. Fibers

Table 1 Viscosity of electrospinning solutions at 25 °C, measured using a rotator viscosity meter

| Solution | Viscosity (mPa s) |
|---|---|
| 30 wt% PU in DMAc | 18 100 |
| Pure glycerol | 1100 |
| 95% glycerol + 5% $H_2O$ | 570 |
| 90% glycerol + 10% $H_2O$ | 307 |
| 85% glycerol + 15% $H_2O$ | 201 |
| 80% glycerol + 20% $H_2O$ | 67 |

 

produced at core–shell phase flow rates of 0.05 : 0.5 mL $h^{-1}$ consisted of approximately 25% solid fibers. Increasing the core phase flow rate to 0.07 and 0.1 mL $h^{-1}$ led to formation of hollow fibers with larger openings (Fig. 1b and c) and a relatively uniform size distribution in the diameter of the fibers (Fig. 1g and h). Further increasing the core phase flow rate beyond 0.15 mL $h^{-1}$, however, mostly led to formation of collapsed hollow fibers (Fig. 1d and e), though the continuous tubular structures were still preserved, presenting a lotus root-like morphology in their cross section. Fiber collapse was thought to mostly occur during the fiber accumulation process. The vapor pressures of DMAc and glycerol at 25 °C are 0.27 kPa and 0.0244 Pa,[40] respectively. Due to the extremely low evaporation rate of glycerol, most of the glycerol will be retained inside the lumen of the nanofibers, therefore nanofibers produced at a high core phase flow rate will be quite heavy. During the continuous electrospinning process, the PU shell of the nanofibers will not be robust enough to endure the pressure from vertically and horizontally overlaid nanofibers. Although the degree of collapse would possibly be reduced by adding polymer to the core solution, formation of core–shell solid fibers, which is not desired, would result.

### 3.2 The effect of the hollow nanofiber structure on the performance of encapsulated enzymes

Convenient control of the structure of the hollow nanofibers provides us with an opportunity to make an in-depth study into the structure–efficiency relationships of hollow-nanofiber based enzymes, which is one of the most important tasks for the advancement of nanobiotechnology. Herein we first prepared hollow PU nanofiber based 3α-HSD and DP separately. The core solutions were prepared by mixing 50 μL water containing pre-dissolved 1 mg 3α-HSD or DP with 950 μL glycerol. By fixing the flow rate of the shell phase solution at 0.5 mL $h^{-1}$ and varying the core phase solution flow rate from 0.05–0.2 mL $h^{-1}$, a series of hollow PU nanofiber based 3α-HSD and DP with different structures were prepared. With bile acid as the substrate and $NAD^+$ as a coenzyme, the activity of 3α-HSD was measured by monitoring the increase in NADH concentration at $OD_{340\ nm}$ ($\varepsilon^{NADH} = 6.22\ mM^{-1}\ cm^{-1}$); the activity of DP was measured using DCPIP as the substrate and NADH as a coenzyme.

Activity recovery of the enzymes encapsulated in the nanofibers was calculated by comparing the specific activity of the encapsulated enzyme with that of the free enzyme. The quantity of enzyme in the membrane sheet used for the activity measurement was calculated using the same method as described previously for the determination of the release percentage of the encapsulated substance. Briefly, for the nanofiber prepared at a core–shell solution flow rate of 0.07 : 0.5 mL $h^{-1}$, for example, the total mass of nanofiber membrane collected after 30 min of stable coelectrospining was approximately 100 mg. Hence the total volume of electrospun core solution will be 0.035 mL (0.07 mL $h^{-1}$ × 0.5 h). Considering the concentration of enzymes in the core solution is 1 mg $mL^{-1}$, and then in total 0.035 mg of enzyme was encapsulated inside 100 mg of membrane. Therefore, the enzyme loading was 0.00035 mg enzyme per mg membrane, and the quantity of enzyme used for the activity measurement could then be calculated by multiplying 0.00035 by the mass of the membrane sheet.

From the above calculation, the relative activity of the enzymes encapsulated in hollow nanofibers prepared at different core–shell phase solution flow rates was determined and the results are presented in Fig. 2. It was found that glycerol was an efficient activator for both 3α-HSD and DP,

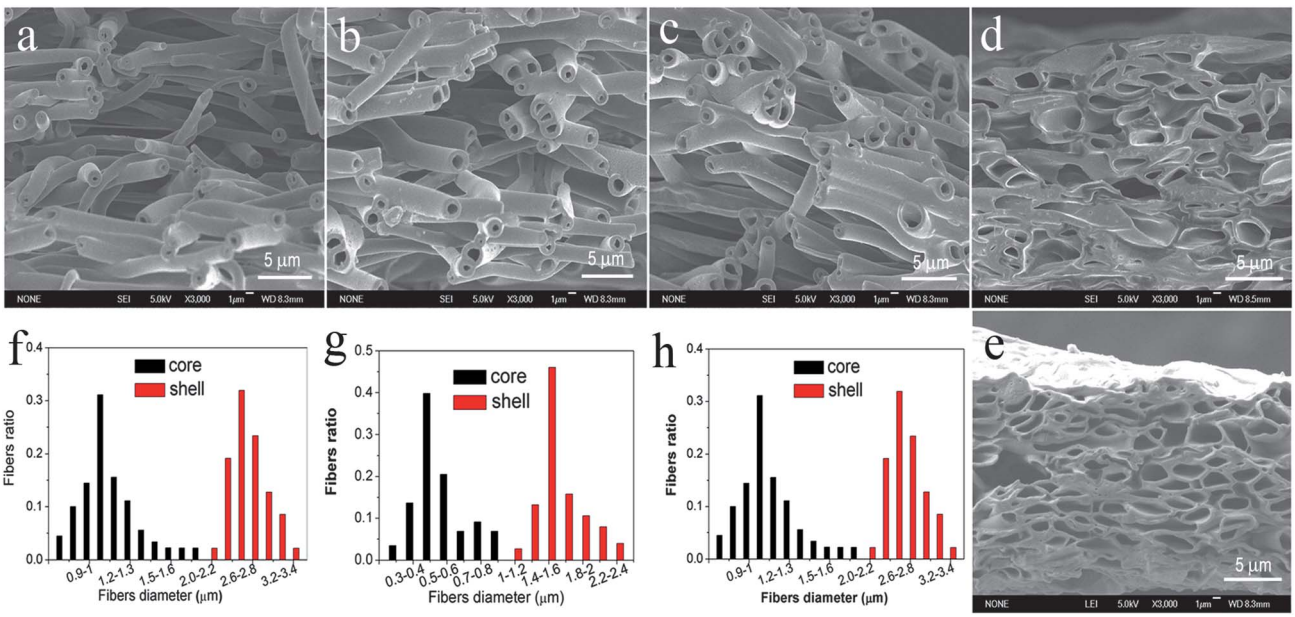


Fig. 1 Hollow nanofibers prepared by co-axial electrospinning. (a–e) Cross-sectional SEM images of hollow nanofibers produced at various core–shell phase solution flow rates: (a) 0.05 : 0.5 mL $h^{-1}$; (b) 0.07 : 0.5 mL $h^{-1}$; (c) 0.1 : 0.5 mL $h^{-1}$; (d) 0.15 : 0.5 mL $h^{-1}$; (e) 0.2 : 0.5 mL $h^{-1}$, (f–h) shows the corresponding size distribution of the inner and outer diameters of the hollow nanofibers shown in images a–c.

approximately 22% and 60% enhancement in the activities of 3α-HSD and DP dissolved in core phase solution were observed. To the best of our knowledge, the activation effect of glycerol on 3α-HSD and DP has not been reported previously.

The structure of the hollow nanofibers influences the activity of the entrapped enzymes significantly; hollow nanofiber based 3α-HSD and DP prepared at a core–shell phase flow rate of 0.07 : 0.5 mL $h^{-1}$ exhibited the highest activity recoveries of 76% and 82%, respectively. Hollow nanofibers produced at higher core phase solution flow rates, however, led to a dramatic decrease in enzyme activity. It has been reported that the activity of the immobilized enzyme depends not only on the chemical composition of the carriers but also on the geometric properties of the carrier such as the shape, size, porosity and pore size distribution.[41,42] Due to the diversity and broad availability of the carriers with different structures, it has been a challenging task to find the most suitable matrix with the desired micro-environment to provide the immobilized enzyme with the highest activity and stability. Results presented in this work suggest that hollow nanofibers with the best defined cylindrical channels fabricated at a core–shell phase flow rate of 0.07 : 0.5 mL $h^{-1}$ provide encapsulated enzymes with the highest activity.

Fig. 3 presents SEM and TEM images of the hollow nanofibers prepared at the core–shell phase flow rate of 0.07 : 0.5 mL $h^{-1}$, as well as a CLSM image of hollow nanofibers containing encapsulated FITC-labelled 3α-HSD as an example. Both Fig. 3(b) and (c) confirm the good dispersion of enzymes inside the lumen of the hollow nanofibers. The high activity of both 3α-HSD and DP encapsulated within the nanofiber prepared at the core–shell phase flow rate of 0.07 : 0.5 mL $h^{-1}$ was largely attributed to the nano-scale shell leading to much reduced mass transfer resistance and a relatively ordered structure. Nevertheless, the lotus root-like nanofibers produced at high core solution flow rates might introduce extra mass transfer resistance to the reactants.

The thermal stability of 3α-HSD and DP was also strongly dependent on the structure of the hollow nanofibers. The results listed in Table 2 show that when 3α-HSD and DP were encapsulated in hollow nanofibers fabricated at a core–shell phase flow rate of 0.07 : 0.5 mL $h^{-1}$, their half lives at 50 °C were enhanced by approximately 40 times compared with their free forms in buffer solution. By comparing the half life of 3α-HSD and DP in the buffer with that in core solution, which consisted of 95% glycerol, we can see that the glycerol in the core solution stabilized the enzymes to a certain extent, this stabilizing mechanism has been reported previously and glycerol has been widely utilized as an enzyme-stabilizing agent.[43,44] However, comparison between the half life of 3α-HSD and DP in buffer with that in hollow nanofibers suggested that the confinement of the enzymes within the nano-scaled microenvironment seems to afford them more significant stabilizing effects.

In the practical application of immobilized enzymes, adsorbing or cross-linking enzyme molecules on a solid surface often exposes the enzyme molecules to harsh conditions, such as hydrophobic interaction with other materials, mechanical sheering and drastic catalytic reaction conditions, which might affect their native structures and activities.[41] As one of the common choices, encapsulation in hollow nanofibers offers several advantages, such as mild synthesis conditions, relatively higher loading capacities and protection of the enzyme molecules from external denaturing factors. Bismuto *et al.*[45] studied the effect of the confinement matrix on the performance of immobilized enzymes, and their results revealed that the enhanced stability was mainly due to the spatial confining effect, which restricts the molecule movement and thus effectively reduces the decomposition of enzyme molecules.

### 3.3 Encapsulation of 3α-HSD, DP and NAD(H) within hollow nanofibers

Measurement of the activities and stabilities of hollow nanofiber-based 3α-HSD and DP indicate that nanofibers produced at a core–shell flow rate of 0.07 : 0.5 mL $h^{-1}$ provide the enzymes with the most suitable microenvironment, consequently, this electrospinning condition was adopted to prepare hollow nanofiber-based multi-enzyme artificial cells for a bile acid assay. As illustrated in Scheme 1, the coupled reaction catalyzed by 3α-HSD and diaphorase could be initiated by using either $NAD^+$ or NADH as the starting coenzyme. Results from the preliminary experiment indicated that using NADH as the

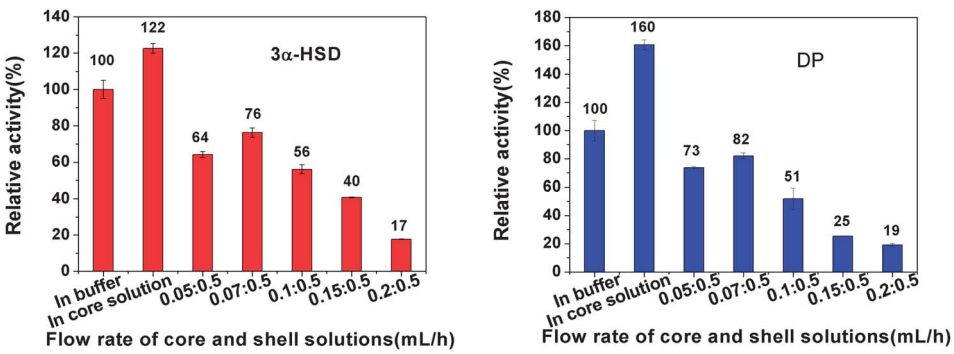


Fig. 2 Relative activities of 3α-HSD and DP in 50 mM Tris-HClbuffer (pH 8.0), in the core phase solution, and in the lumen of the PU hollow nanofiber produced at different core–shell phase solution flow rates. Activities of enzymes in 50 mM Tris-HClbuffer (pH 8.0) are normalized as 100%.

 

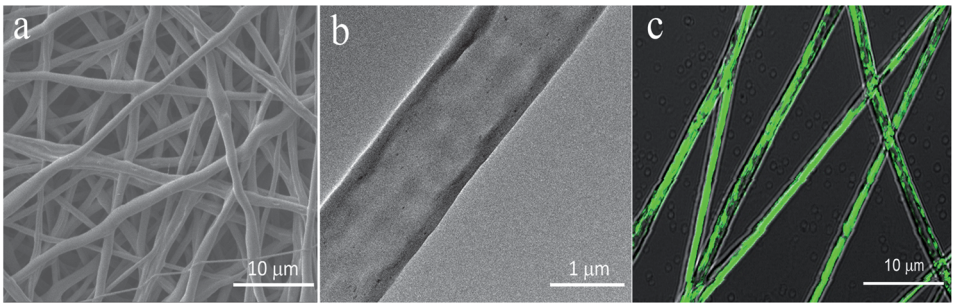


Fig. 3 Hollow nanofibers produced at a core–shell flow rate of 0.07 : 0.5 mL $h^{-1}$ with encapsulated enzymes. (a) SEM image of as-spun hollow nanofibers, (b) TEM image of as-spun hollow nanofibers, and (c) CLSM image of hollow nanofibers with encapsulated 3α-HSD that had been labelled with FITC.

Table 2 Half life ($T_{1/2}$) of 3α-HSD and DP at 50 °C in free formations and encapsulated in the lumen of PU hollow nanofibers produced at different core–shell phase flow rates

| Enzyme | $T_{1/2}$ in buffer (h) | $T_{1/2}$ in core solution (h) | $T_{1/2}$ of enzyme encapsulated in hollow nanofibers[a] (h) | | | | |
|---|---|---|---|---|---|---|---|
| | | | a | b | c | d | e |
| 3α-HSD | 2.30 | 3.28 | 79 | 89 | 68 | 40 | 17 |
| DP | 1.30 | 1.95 | 45 | 49 | 40 | 35 | 27 |

[a] Hollow nanofibers were produced at core–shell phase flow rates of a: 0.05 : 0.5 mL $h^{-1}$, b: 0.07 : 0.5 mL $h^{-1}$, c: 0.1 : 0.5 mL $h^{-1}$, d: 0.15 : 0.5 mL $h^{-1}$, and e: 0.2 : 0.5 mL $h^{-1}$.

starting coenzyme resulted in a higher reaction rate than that using $NAD^+$ as the starting coenzyme (data were not shown). With NADH as the coenzyme, DP catalyzed the reduction of DCPIP to form a colourless product, resulting in a decrease in absorbance at 600 nm; the 3α-HSD catalyzed bile acid oxidation could then facilitate regeneration of the oxidized coenzyme to NADH, consequently, the rate of DP reduction was accelerated. By measuring the rate of DCPIP reduction in terms of $\Delta A_{600\ nm}$/min per mg enzyme per mL over a range of bile acid concentrations, a standard curve for bile acid assay was obtained. Fig. 4 presents the standard curves obtained using hollow nanofiber-based artificial cells which were prepared by co-axial electrospinning with a core phase solution containing 1 mg $mL^{-1}$ 3α-HSD, 1 mg $mL^{-1}$ DP and 50 mg $mL^{-1}$ NADH, and 30% PU as shell solution at a core–shell flow rate of 0.07 : 0.5 mL $h^{-1}$. For each measurement, approximately 4 mg 'as-electrospun' nanofibrous membrane was immersed into 2 mL reactant mixture solution to initiate the coupled reaction.

Using this nanofiber-based artificial cell, a good linear increase in reaction rate was observed, until the reaction rate reach a plateau at high bile acid concentrations (>200 μM). The linear range was slightly broader than that obtained by using the solution-based multi-enzyme system with concentrations of 3α-HSD, DP and NADH which were the same as that for the hollow nanofiber-based systems. By comparing the reaction rates of the DCPIP reduction catalyzed by these two different multi-enzyme systems at a bile acid concentration of 150 μM, the apparent lumped activity recovery of the hollow-nanofiber based artificial cell was calculated to be approximately 75.0%. This reaction rate was slightly higher than that measured with co-immobilized 3α-HSD and DP, but with added free NADH. Considering that most reported immobilized coenzyme systems could hardly maintain their reactivity above 1% of their solution counterpart,[18,20] the overall activity yield achieved with this novel hollow nanofiber-based artificial cell was considered to be exciting. Coenzyme-dependent biotransformations require a readily dissociable cofactor. Within the nanofiber-based artificial cell, both the enzymes and the coenzymes remained in free formations inside the lumen of the hollow fiber. The translocation of the cofactor between the two enzymes was therefore essentially retained, or even facilitated within the nano-scale environment due to the enhanced interaction frequency between the enzymes and the coenzymes.

The high activity of the hollow-nanofiber artificial cell also benefited from the high diffusion rate of the reactant. Release tests indicated that the hollow nanofiber wall has a characteristic molecular weight cut-off at approximately 20 kDa (Fig. 5). When substances with a molecular weight less than 20 kDa, *i.e.*, glycerol, NADH, protamine, and lysozyme were encapsulated within the hollow nanofiber, approximately 60% of the encapsulated substance was released into the buffer solution within 1 min, suggesting a very fast diffusion rate. However, when enzymes with a molecular weight larger than 20 kDa, like 3α-HSD and DP, were encapsulated no detectable release was observed, even when the test was carried out with nanofibers that had been frozen and broken to pieces as small as possible exposing the openings of the hollow fibers as much as possible. This feature was thought to be greatly advantageous over other kinds of materials with exposed surfaces for enzyme immobilization. It should be pointed that although approximately 90% of the encapsulated NADH was released into the buffer solution within 5 min, the result shown in Fig. 4 indicates that the co-encapsulation of NADH along with 3α-HSD and DP still imposed some synergistic effects on the coupled reaction, as confirmed by the slightly higher reaction rate than that which was obtained with co-immobilized 3α-HSD and DP, with free NADH. This was probably because the reaction rate was determined within 3 min, therefore a slightly higher local concentration of NADH was present inside the lumen for the artificial system.

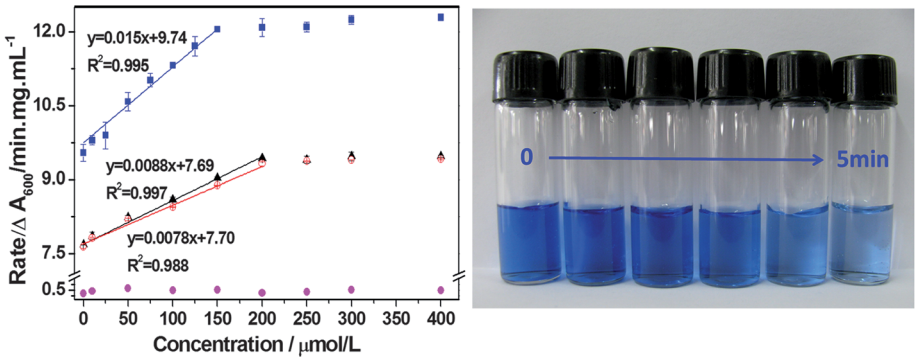


Fig. 4 Calibration curves for the bile acid assay obtained by using multi-enzyme systems consisting of 3α-HSD, DP and NADH in different forms. (■) Free multi-enzymes and NADH, (▲) nanofiber-based artificial cell, (○) co-immobilized 3α-HSD and DP with added free NADH, (●) blank hollow nanofibers. Concentrations of enzyme and coenzyme for all measurements were same. Picture on the right shows colour changes during measurement after removing the nanofibrous artificial cell at different times, for a better view, 10 mg membrane was added to 2 mL reactant solution.

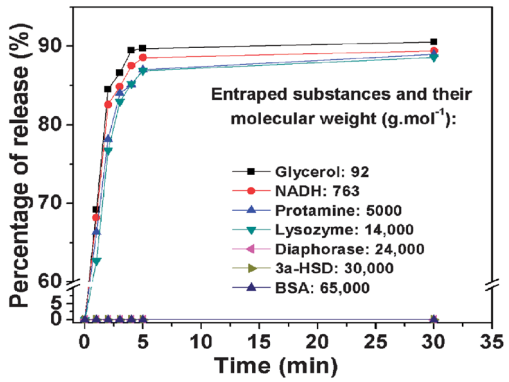


Fig. 5 Release of individually encapsulated substances from hollow nanofiber produced at a core–shell phase flow rate of 0.07 : 0.5 mL $h^{-1}$.

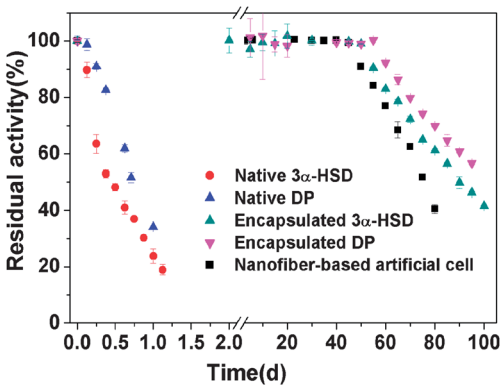


Fig. 6 Stability of free and the individually encapsulated 3α-HSD and DP, as well as the stability of nanofiber-based multi-enzyme artificial cells involving co-encapsulated 3α-HSD, DP and NADH for bile acid assay at 25 °C. The enzyme-containing hollow nanofibers were all produced at a core–shell phase flow rate of 0.07 : 0.5 mL $h^{-1}$.

Encapsulation greatly stabilized the enzymes. We firstly checked the stability of the individually encapsulated 3α-HSD and DP in hollow nanofibers that were prepared at a core–shell phase flow rate of 0.07 : 0.5 mL $h^{-1}$. The results in Fig. 6 show that the half lives of the individually encapsulated 3α-HSD and DP were as long as 90 and 110 days at 25 °C, corresponding to 183 and 174 times enhancement compared with their native formations. The hollow nanofiber-based artificial cells involving co-encapsulated 3α-HSD, DP and NADH for the bile acid assay also presented an extraordinarily long half life of 76 day at 25 °C. It is known that NADH is also easily loses its activity, especially in low pH solutions due to the acid-catalyzed hydration reaction of NADH.[46] We measured the stability of NADH both in 50 mM Tris-HCl buffer (pH 8.0), where the enzyme assay was performed, and in the core solution used for co-axial electrospinning. The half life of NADH in the two solutions above was determined to be 23.74 days and 25.02 days, respectively, at 25 °C. Considering the long half life of the artificial cell (76 days), it could be reasonably speculated that the stability of NADH was also significantly improved after encapsulation. This excellent storage stability makes the prepared nanofiber based artificial cell attractive for potential clinic applications.

## 4. Conclusions and future perspectives

In summary, we have shown that a novel hollow nanofiber based artificial cell that perform multi-step reactions involving coenzyme regeneration efficiently was successfully fabricated *in situ* by a facile co-axial electrospinning process. This brand-new design for artificial cells afforded high performance multi-enzymatic biotransformations and greatly overcame the limitations of traditional particle-based multi-enzyme systems. The multi-enzyme system in the current study was for single-use bioassay, which meant the measurement was negligibly affected by the quick release of the low-molecular weight coenzyme from the nanofiber. For biotransformations that require the immobilized multi-enzyme system to be repeatedly used, macromolecularization of the coenzyme, which was extensively studied in 1980's will provide an efficient solution to avoid the quick release of small molecule coenzymes,[47] considering the nanofiber wall showed a characteristic molecular weight cut-off about 20 kDa.

 

More recently, fabrication and application of bioactive particles with multicompartments was regarded as a key requirement for the development of next-generation carriers because these systems combine physicochemical properties that are not readily achievable using single component assemblies.[10,11,17,48] Multi-channel tubes with up to five channels were successfully prepared using a multifluidic compound-jet electrospinning technique by using paraffin oil as the core liquid, ethanol solution of $Ti(OiPr)_4$ and poly(vinyl pyrrolidone) as the shell liquid.[29,30] The same research group also reported preparation of bi-component microcapsules *via* a similar compound-fluidic electrospray process.[49] By replacing the core liquid with a glycerol solution of different enzymes and the shell liquid with DMAc solutions of PU, multi-channel nanofibers would be created, so that it could be possible to assemble different enzymes and coenzymes separately into each separated nanochannel. It was believed that results from this study will greatly promote and broaden the application of multi-enzyme systems in industry, biosensing, biomedicine and many other related research fields.

## Acknowledgements

The support from the 973 program (2009CB724705) and National Natural Science Foundation of China (Grant no. 20976180, 21376249) is kindly acknowledged.

## References

1 K. F. Gu and T. M. S. Chang, *Biotechnol. Bioeng.*, 1990, **36**, 263–269.
2 J. Shi, X. Wang, W. Zhang, Z. Jiang, Y. Liang, Y. Zhu and C. Zhang, *Adv. Funct. Mater.*, 2013, **23**, 1450–1458.
3 B. W. Park, D. Y. Yoon and D. S. Kim, *Biosens. Bioelectron.*, 2010, **26**, 1–10.
4 Y. Zhang, W. C. Ruder and P. R. LeDuc, *Trends Biotechnol.*, 2008, **26**, 14–20.
5 P. Tanner, S. Egli, V. Balasubramanian, O. Onaca, C. G. Palivan and W. Meier, *FEBS Lett.*, 2011, **585**, 1699–1706.
6 T. M. S. Chang, *Science*, 1964, **146**, 524–525.
7 T. M. S. Chang, *Nature*, 1971, **229**, 117–118.
8 T. M. S. Chang, *Methods Enzymol.*, 1985, **112**, 195–203.
9 T. M. S. Chang and S. Prakash, *Mol. Biotechnol.*, 2001, **17**, 249–260.
10 A. M. Yashchenok, M. Delcea, K. Videnova, E. A. Jares-Erijman, T. M. Jovin, M. Konrad, H. Möhwald and A. G. Skirtach, *Angew. Chem., Int. Ed.*, 2010, **49**, 8116–8120.
11 R. Chandrawati, P. D. Odermatt, S.-F. Chong, A. D. Price, B. Stadler and F. Caruso, *Nano Lett.*, 2011, **11**, 4958–4963.
12 R. Chandrawati, M. P. van Koeverden, H. Lomas and F. Caruso, *J. Phys. Chem. Lett.*, 2011, **2**, 2639–2649.
13 D. M. Vriezema, P. M. Garcia, N. Sancho Oltra, N. S. Hatzakis, S. M. Kuiper, R. J. Nolte, A. E. Rowan and J. van Hest, *Angew. Chem.*, 2007, **119**, 7522–7526.
14 A. Blanazs, S. P. Armes and A. J. Ryan, *Macromol. Rapid Commun.*, 2009, **30**, 267–277.
15 S. F. van Dongen, W. P. Verdurmen, R. J. Peters, R. J. Nolte, R. Brock and J. van Hest, *Angew. Chem., Int. Ed.*, 2010, **49**, 7213–7216.
16 R. J. Peters, I. Louzao and J. C. van Hest, *Chem. Sci.*, 2012, **3**, 335–342.
17 S. T. Retterer and M. L. Simpson, *Curr. Opin. Biotechnol.*, 2012, **23**, 522–528.
18 B. El-Zahab, H. Jia and P. Wang, *Biotechnol. Bioeng.*, 2004, **87**, 178–183.
19 J. Rocha-Martín, B. d. l. Rivas, R. Munoz, J. M. Guisán and F. López-Gallego, *ChemCatChem*, 2012, **4**, 1279–1288.
20 B. El-Zahab, D. Donnelly and P. Wang, *Biotechnol. Bioeng.*, 2008, **99**, 508–514.
21 W. Liu, S. Zhang and P. Wang, *J. Biotechnol.*, 2009, **139**, 102–107.
22 Y. Zhang, F. Gao, S. P. Zhang, Z. G. Su, G. H. Ma and P. Wang, *Bioresour. Technol.*, 2011, **102**, 1837–1843.
23 M. Zheng and S. Zhang, *Biocatal. Biotransform.*, 2011, **29**, 278–287.
24 I. G. Loscertales, A. Barrero, I. Guerrero, R. Cortijo, M. Marquez and A. Ganan-Calvo, *Science*, 2002, **295**, 1695–1698.
25 I. G. Loscertales, A. Barrero, M. Márquez, R. Spretz, R. Velarde-Ortiz and G. Larsen, *J. Am. Chem. Soc.*, 2004, **126**, 5376–5377.
26 D. Li and Y. Xia, *Nano Lett.*, 2004, **4**, 933–938.
27 J. T. McCann, D. Li and Y. Xia, *J. Mater. Chem.*, 2005, **15**, 735–738.
28 D. Li, J. T. McCann, Y. Xia and M. Marquez, *J. Am. Ceram. Soc.*, 2006, **89**, 1861–1869.
29 Y. Zhao, X. Cao and L. Jiang, *J. Am. Chem. Soc.*, 2007, **129**, 764–765.
30 Y. Zhao and L. Jiang, *Adv. Mater.*, 2009, **21**, 3621–3638.
31 J. Kim, J. W. Grate and P. Wang, *Chem. Eng. Sci.*, 2006, **61**, 1017–1026.
32 P. Wang, *Curr. Opin. Biotechnol.*, 2006, **17**, 574–579.
33 Z. G. Wang, L. S. Wan, Z. M. Liu, X. J. Huang and Z. K. Xu, *J. Mol. Catal. B: Enzym.*, 2009, **56**, 189–195.
34 N. T. Daniel and K. J. Balkus Jr, *Top. Catal.*, 2012, **55**, 1057–1069.
35 Z. Kurban, A. Lovell, S. M. Bennington, D. W. Jenkins, K. R. Ryan, M. O. Jones, N. T. Skipper and W. I. David, *J. Phys. Chem. C*, 2010, **114**, 21201–21213.
36 Z. Sun, E. Zussman, A. L. Yarin, J. H. Wendorff and A. Greiner, *Adv. Mater.*, 2003, **15**, 1929–1932.
37 J. H. Yu, S. V. Fridrikh and G. C. Rutledge, *Adv. Mater.*, 2004, **16**, 1562–1566.
38 T. T. T. Nguyen, O. H. Chung and J. S. Park, *Carbohydr. Polym.*, 2011, **86**, 1799–1806.
39 Y. Zhang, Z.-M. Huang, X. Xu, C. T. Lim and S. Ramakrishna, *Chem. Mater.*, 2004, **16**, 3406–3409.
40 H. K. Cammenga, F. W. Schulze and W. Theuerl, *J. Chem. Eng. Data*, 1977, **22**, 131–134.
41 L. Cao, L. v. Langen and R. A. Sheldon, *Curr. Opin. Biotechnol.*, 2003, **14**, 387–394.

42 J. Aparicio and J. Sinisterra, *J. Mol. Catal.*, 1993, **80**, 269–276.
43 S. L. Bradbury and W. B. Jakoby, *Proc. Natl. Acad. Sci. U. S. A.*, 1972, **69**, 2373–2376.
44 V. Vagenende, M. G. Yap and B. L. Trout, *Biochemistry*, 2009, **48**, 11084–11096.
45 E. Bismuto, P. L. Martelli, A. De Maio, D. G. Mita, G. Irace and R. Casadio, *Biopolymers*, 2002, **67**, 85–95.
46 S. L. Johnson and P. T. Tuazon, *Biochemistry*, 1977, **16**, 1175–1183.
47 A. F. Bückmann and G. Carrea, *Adv. Biochem. Eng./Biotechnol.*, 1989, **39**, 97–152.
48 M. Delcea, A. Yashchenok, K. Videnova, O. Kreft, H. Möhwald and A. G. Skirtach, *Macromol. Biosci.*, 2010, **10**, 465–474.
49 H. Chen, Y. Zhao, Y. Song and L. Jiang, *J. Am. Chem. Soc.*, 2008, **130**, 7800–7801.